



Total Ionizing Dose Test Report

No. 11T-RT1280FP5986501

July 22, 2011

Table of Contents

I.	Summary Table.....	3
II.	Total Ionizing Dose (TID) Testing.....	3
A.	Device Under Test (DUT).....	3
B.	Irradiation	3
C.	Test Method	4
D.	Electrical Parameter Measurements.....	4
III.	Test Results	5
A.	Functional Test.....	5
B.	Influx and Post-Annealing ICC.....	5
C.	Input Logic Threshold.....	9
D.	Output Characteristic	10
E.	Propagation Delays.....	11
F.	Transient Characteristics	12

TOTAL IONIZING DOSE TEST REPORT

No. 11T-RT1280-FP5986501

July 22, 2011

C.K. Huang and J.J. Wang

(650) 318-4209, (650) 318-4576

chang-kai.huang@microsemi.com, jih-jong.wang@microsemi.com

I. Summary Table

Parameters	Tolerance
1. Gross Functional	Pass 8 krad(SiO ₂)
2. I _{DDSTDBY}	Pass 5 krad(SiO ₂), will pass 8 krad(SiO ₂) after annealing
3. VIL/VIH	Pass 8 krad(SiO ₂)
4. VOL/VOH	Pass 8 krad(SiO ₂)
5. Propagation Delays	Pass 8 krad(SiO ₂)
6. Rising/Falling Edge Transient	Pass 8 krad(SiO ₂)

II. Total Ionizing Dose (TID) Testing

This section describes the device under test (DUT), the irradiation parameters, the test method and the test parameters.

A. Device Under Test (DUT)

Table 1 lists the DUT information.

Table 1 DUT Information

Part Number	RT1280
Package	CQFP172
Foundry	MEC
Technology	0.8 um CMOS
Die Lot Number	FP5986501

B. Irradiation

Table 2 lists the irradiation parameters.

Table 2 Irradiation Parameters

Facility	DMEA
Radiation Source	Co-60
Dose Rate	1 krad(SiO ₂)/min ($\pm 5\%$)
Data Mode	Static
Temperature	Room
Bias	5.0 V

C. Test Method

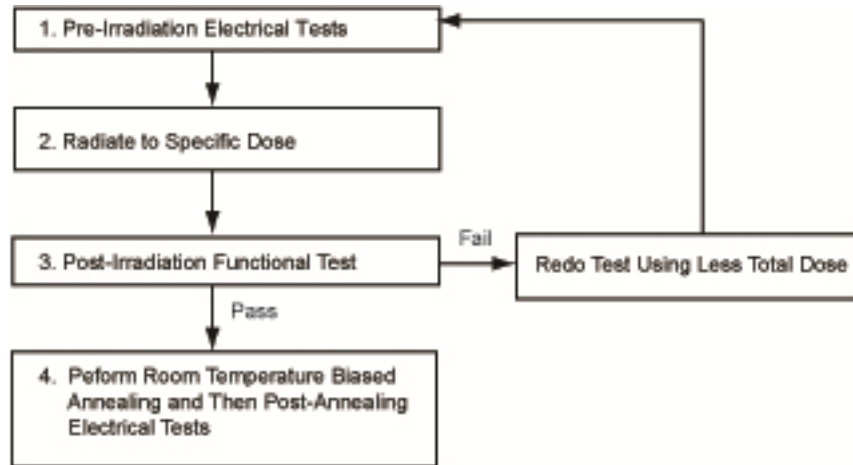


Figure 1 TID Test Flow Chart

The test method basically is in compliance with the military standard TM1019.8. Figure 1 is the flow chart of the testing sequence. The accelerated annealing test in section 3.12 is not performed lot-to-lot. This is because for the CMOS technology used by the RT1280 product, the adverse effects due to interface state at the gate SiO₂/Si interface are negligible, and the dominant annealing effect in this device is the reduction of trapped holes in the SiO₂. So the accelerated annealing basically alleviates the radiation effects on the DUT.

Section 3.11 extended room temperature annealing test is also applied. Room temperature annealing for approximately 5 days was done on each device before the final parameter measurements.

D. Electrical Parameter Measurements

The electrical parameters were measured on the bench. Compared to an automatic tester, this bench setup has less noise, while it samples selected pins for threshold voltage measurements. However, the conservative dose level used to measure the parameters usually is too low to show any threshold voltage changes. ICC usually dictates the dose level for parameter measurements, and consequently determines the radiation tolerance. Thus sampling few pins is sufficient to prove that the radiation effects at the measured level cause no concerns on the threshold voltages. Other advantages for this bench setup are the influx measurement of ICC and the measurement of the signal transient characteristic. Table 3 lists the corresponding logic design for each electrical measurement.

Table 3 Logic Design for each Measured Parameter

Parameter/Characteristics	Logic Design
1. Functionality	All key architectural functions
2. ICC	DUT power supply
3. VIL/VIH	TTL compatible input buffer
4. VOL/VOH	TTL compatible output buffer
5. Propagation Delays	String of inverters
6. Rising/Falling Edge	TTL compatible output

III. Test Results

A. Functional Test

Referring to Figure 1, the post irradiation functional test is performed on one I/O design. Since the functionality versus total dose is determined by the TID tolerance of the charge pump, this test provides a fast and effective test for on-site post-irradiation functional test. The post annealing functional test is performed on key architectural functions includes I/O, combinational logic, and shift registers.

Every DUT passed the post-irradiation and post-annealing functional tests.

B. Influx and Post-Annealing ICC

Table 4 Pre-Irradiation, Post-Irradiation and Post-Annealing ICC

DUT	Total Dose krad(SiO ₂)	ICC (mA)		
		Pre-irrad	Post-irrad	Post-ann
1301	8	0.11	136	71
1328	8	0.11	138	68
1342	8	0.12	119	72
1369	8	0.11	135	76
1413	8	0.11	123	74

Figure 2 to Figure 6 show the influx ICC. All 5 DUTs would pass the ICC specification after 5 krad(SiO₂) of irradiation.

As shown in Table 4, also, after 5 days of annealing the 8 krad(SiO₂) DUTs did not have ICC lowered within the specification of 25 mA. Additional annealing was applied to 3 DUTs for the projection, as shown in Figure 7.

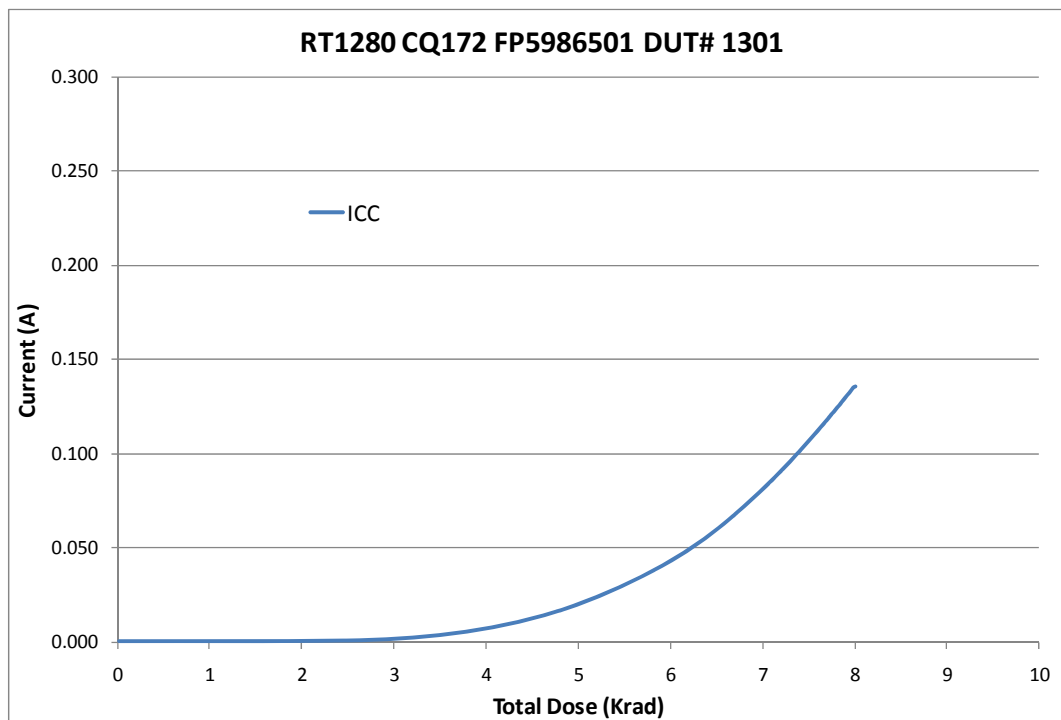


Figure 2 DUT 1301 Influx ICC

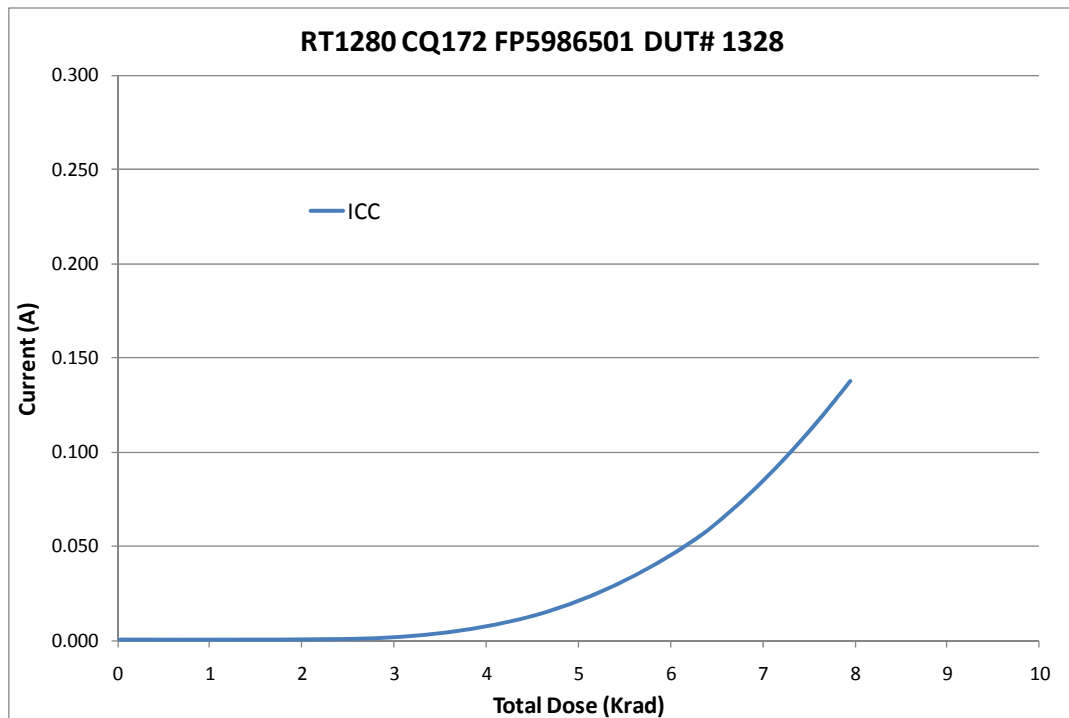


Figure 3 DUT 1328 Influx ICC

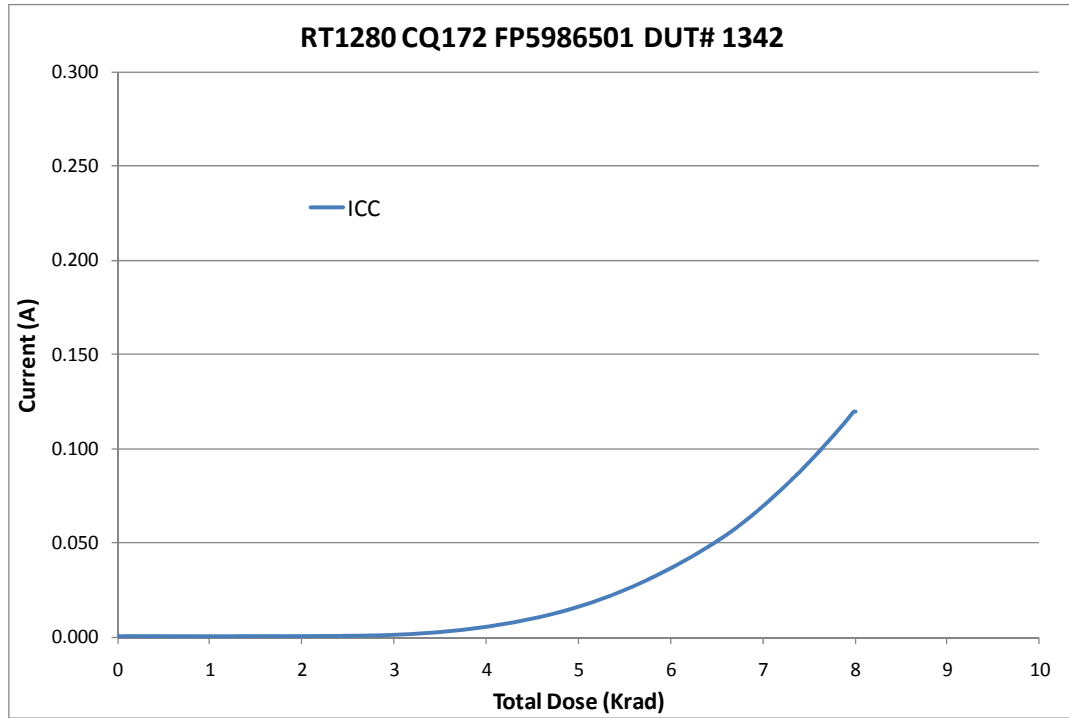


Figure 4 DUT 1342 Influx ICC

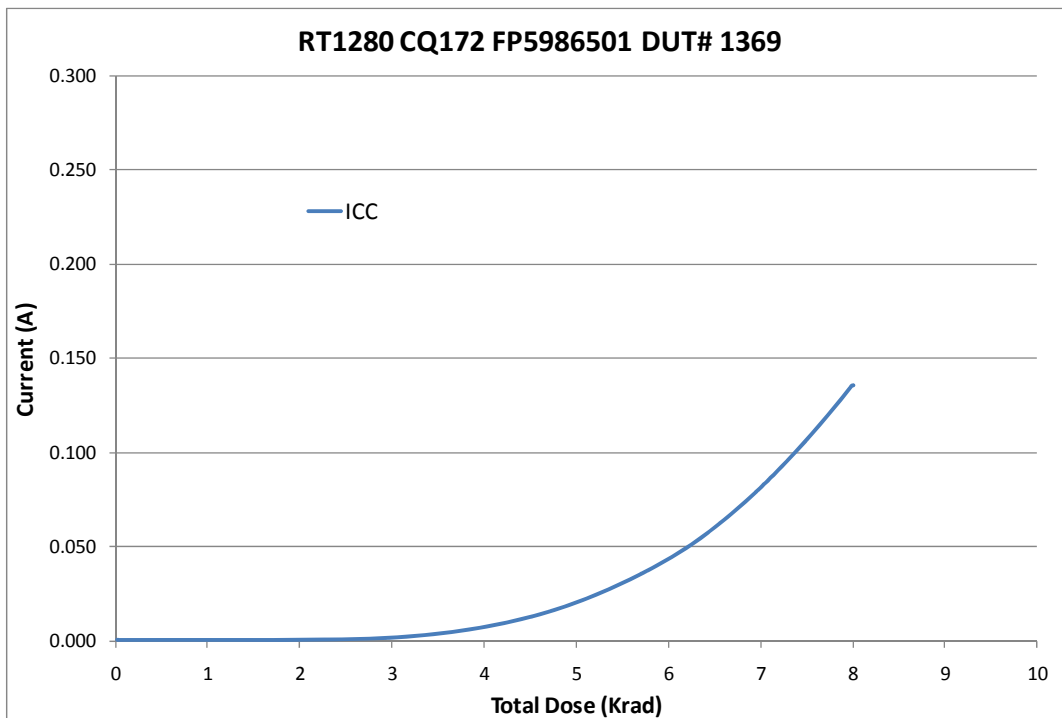


Figure 5 DUT 1369 Influx ICC

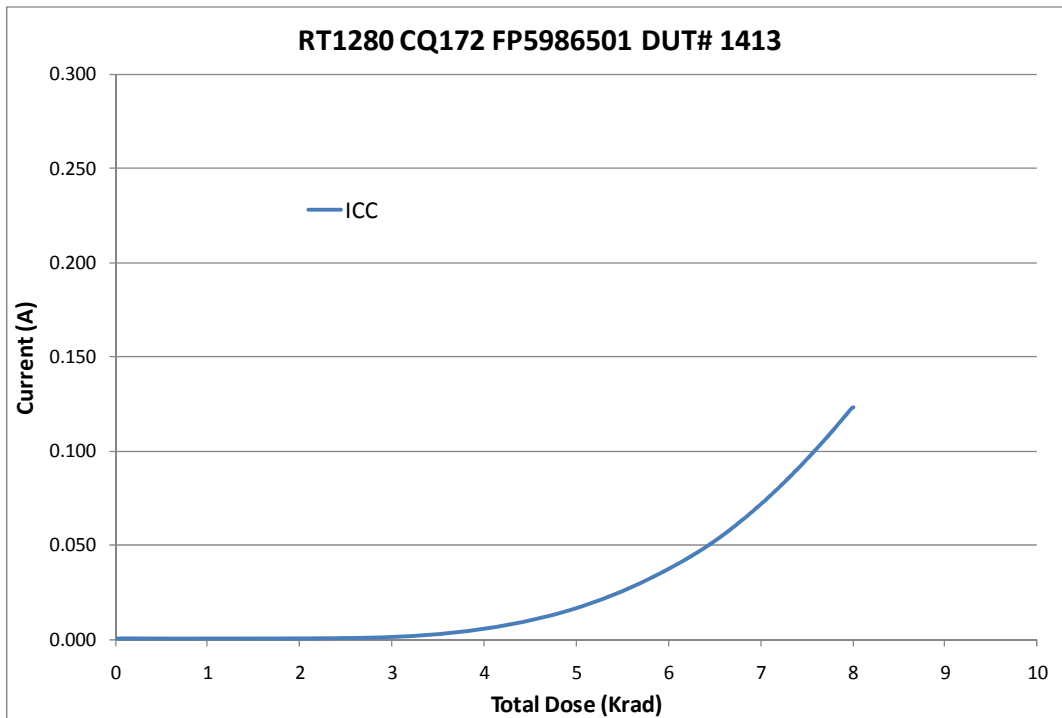


Figure 6 DUT 1413 Influx ICC

Although the post annealing ICC of 8 krad(SiO₂)-DUT did not reduce to within the specification of 25 mA after 5 days, it is expected that longer annealing will meet the specification after about 200 days from the trendline shown in Figure 7.

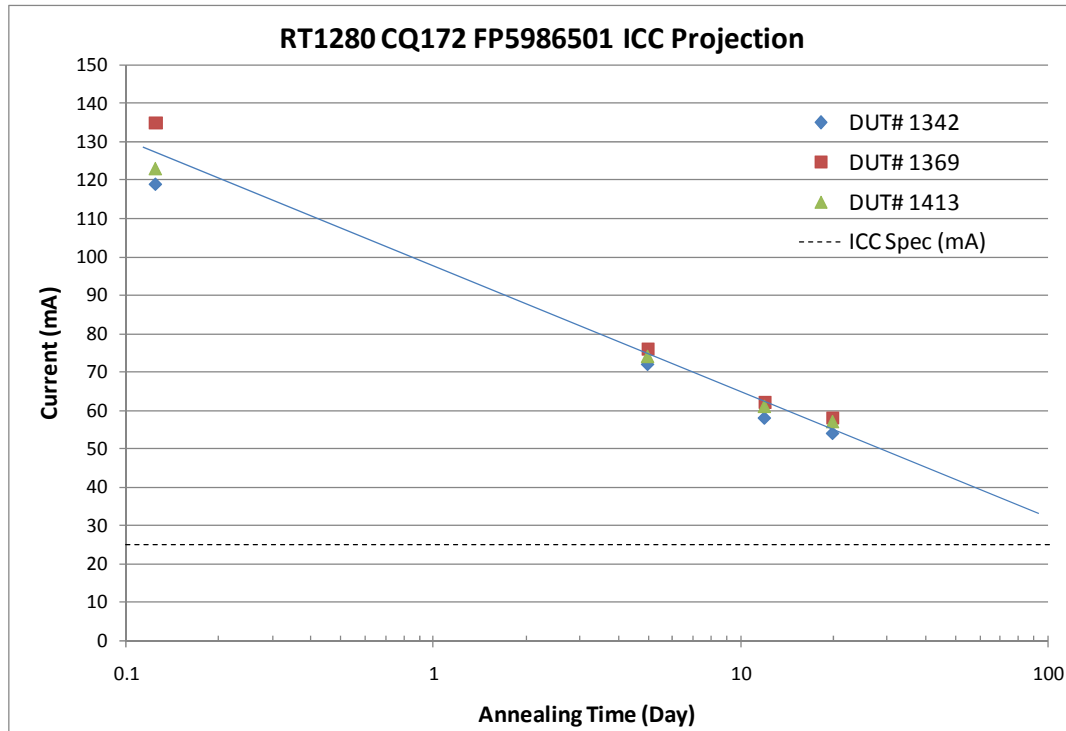


Figure 7 Annealing Effect to ICC

C. Input Logic Threshold

Table 5 lists the input logic threshold of each DUT for pre-irradiation and post-annealing; all data is within the specification.

Table 5 Input Logic Threshold (VIL/VIH) Results (V)

DUT	Total Dose krad(SiO ₂)	VIL (V)		VIH (V)	
		Pre-Irrad	Post-Ann	Pre-Irrad	Post-Ann
1301	8	1.265	1.278	1.231	1.241
1328	8	1.268	1.287	1.230	1.251
1342	8	1.264	1.284	1.225	1.249
1369	8	1.281	1.291	1.241	1.254
1413	8	1.279	1.293	1.241	1.256

D. Output Characteristic

Table 6a and Table 6b show the VOL characteristics for the pre-irradiated and post-annealed DUT; all data is within the specification. The specification is that when $I_{OL} = 6 \text{ mA}$, VOL cannot exceed 0.4 V.

Table 6a VOL for various drive currents (mV)

Current (mA)	DUT 1301		DUT 1328		DUT 1342	
	Pre-Irrad (mV)	Post-Ann (mV)	Pre-Irrad (mV)	Post-Ann (mV)	Pre-Irrad (mV)	Post-Ann (mV)
1	22	23	21	23	22	22
5	110	111	108	111	109	111
10	222	224	218	223	220	224
20	454	459	446	451	449	459

Table 6b VOL for various drive currents (mV)

Current (mA)	DUT 1369		DUT 1413	
	Pre-Irrad (mV)	Post-Ann (mV)	Pre-Irrad (mV)	Post-Ann (mV)
1	22	23	22	23
5	109	112	109	113
10	220	225	219	229
20	449	456	448	471

Table 7a and Table 7b show the VOH characteristic curves for the pre-irradiated and post-annealed DUT; all data is within the specification. The specification is that when $I_{OH} = 4 \text{ mA}$, VOH cannot be lower than 3.7 V.

Table 7a VOH for Various Drive Currents (V)

Current (mA)	DUT 1301		DUT 1328		DUT 1342	
	Pre-Irrad	Post-Ann	Pre-Irrad	Post-Ann	Pre-Irrad	Post-Ann
1	4.9683	4.9642	4.9684	4.9661	4.9709	4.9728
5	4.7048	4.6924	4.7082	4.7003	4.7182	4.7134
10	4.3532	4.3292	4.3622	4.3485	4.3830	4.3701
20	3.4149	3.3271	3.4641	3.4463	3.5264	3.4530

Table 7b VOH for Various Drive Currents (V)

Current (mA)	DUT 1369		DUT 1413	
	Pre-Irrad	Post-Ann	Pre-Irrad	Post-Ann
1	4.9681	4.9630	4.9711	4.9673
5	4.7047	4.6921	4.7182	4.7072
10	4.3532	4.3321	4.3822	4.3594
20	3.4152	3.3452	3.5193	3.4421

E. Propagation Delays

Table 8 lists the pre-irradiation and post-annealing propagation delays. The results show small radiation effects; in any case, the percentage change is below $\pm 10\%$.

Table 8 Radiation-Induced Propagation Delay Degradations

DUT	Total Dose krad(SiO ₂)	Pre-Irradiation (ns)	Post-Irradiation (ns)	Post-Annealing (ns)	Degradation (%)
1301	8	1380.0	1416.1	1405.6	1.86%
1328	8	1367.6	1415.8	1368.2	0.04%
1342	8	1360.8	1408.2	1346.5	-1.05%
1369	8	1376.0	1431.1	1397.5	1.56%
1413	8	1353.3	1389.3	1364.3	0.81%

F. Transient Characteristics

The rising and falling edge transient of an output is measured pre-irradiation and post-annealing. Figure 8a to Figure 17b show the pre-irradiation and post-annealing transition edges. In each case, the radiation-induced transition-time degradation is not observable.

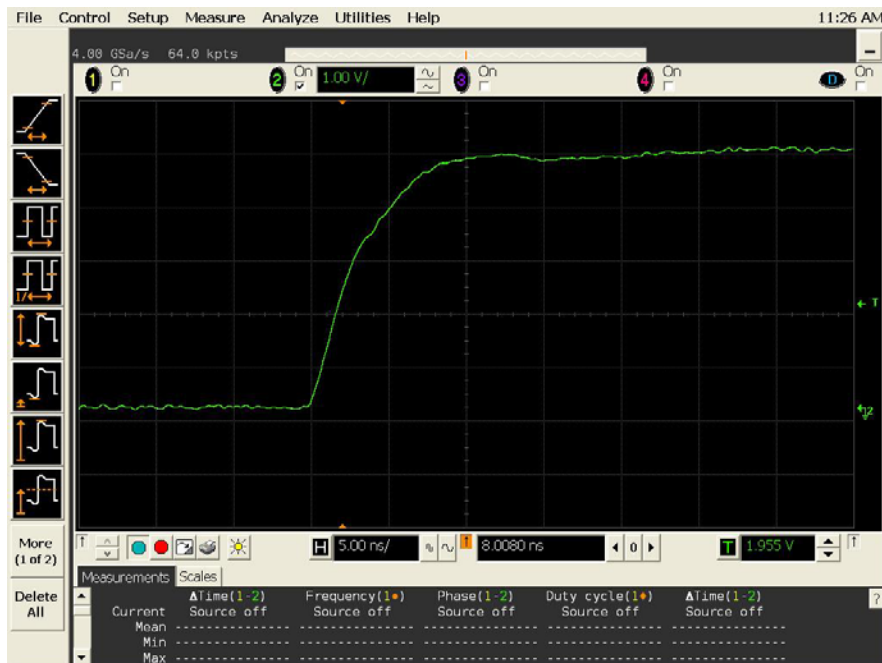


Figure 8a DUT 1301 Pre-Irradiation Rising Edge,
abscissa scale is 1 V/div and ordinate scale is 5 ns/div.



Figure 8(b) DUT 1301 Post-Annealing Rising Edge,
abscissa scale is 1 V/div and ordinate scale is 5 ns/div.

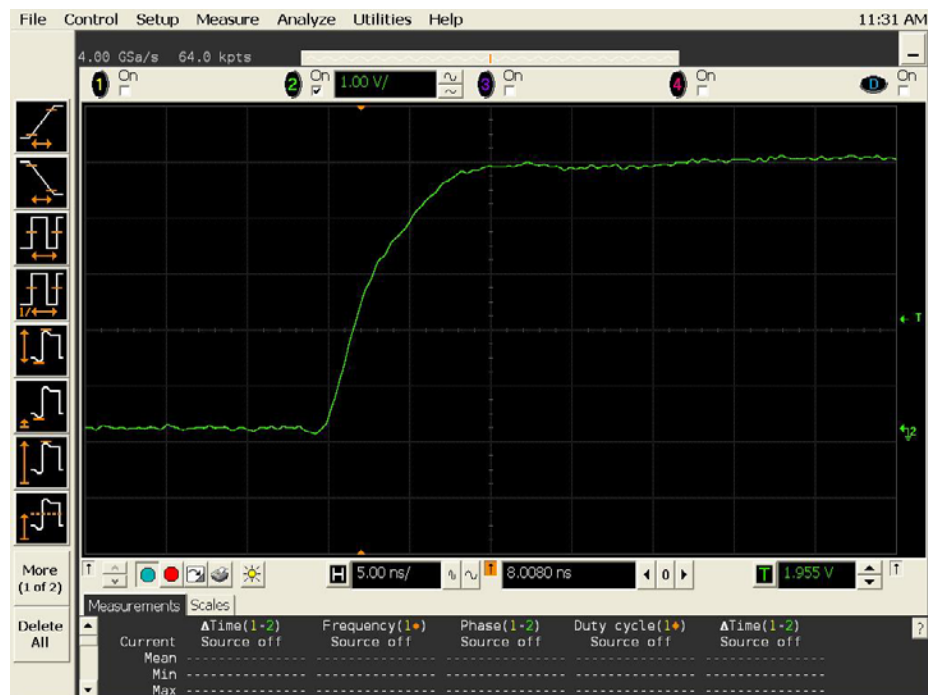


Figure 9a DUT 1328 Pre-Irradiation Rising Edge,
abscissa scale is 1 V/div and ordinate scale is 5 ns/div.



Figure 9b DUT 1328 Post-Annealing Rising Edge,
abscissa scale is 1 V/div and ordinate scale is 5 ns/div.

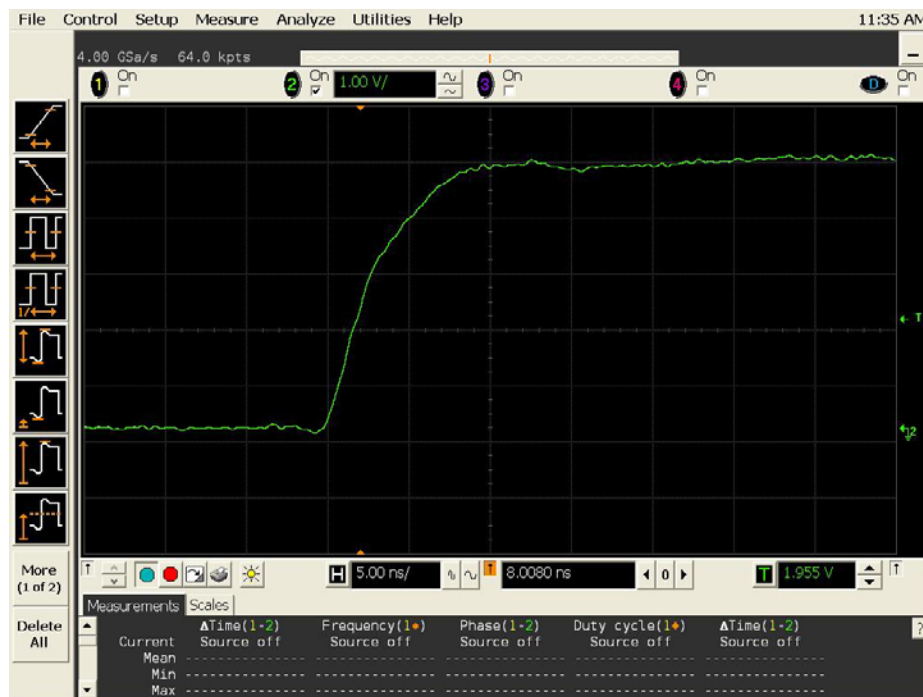


Figure 10a DUT 1342 Pre-Radiation Rising Edge,
abscissa scale is 1 V/div and ordinate scale is 5 ns/div.

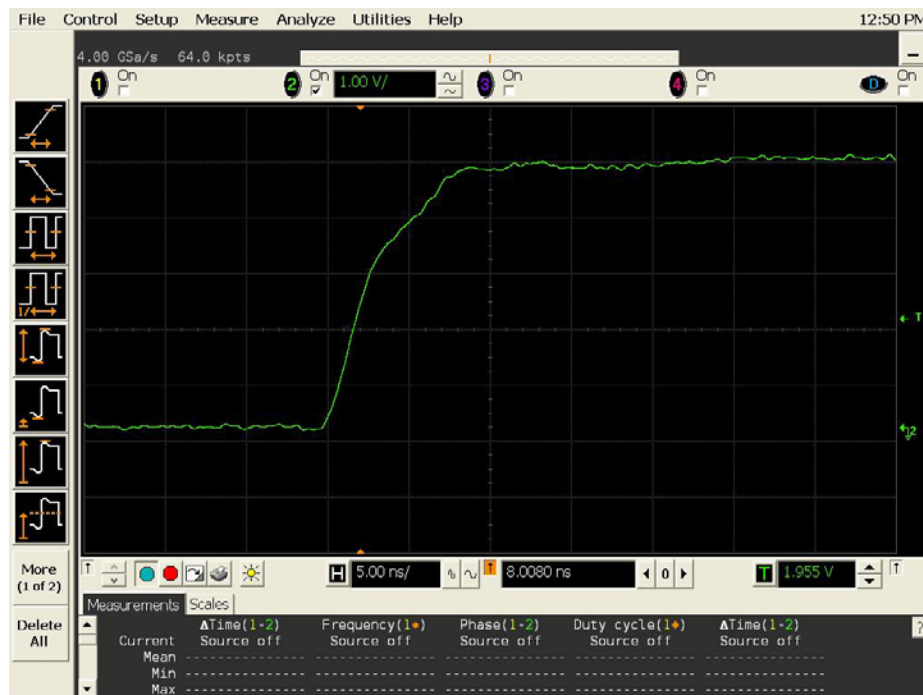


Figure 10b DUT 1342 Post-Annealing Rising Edge,
abscissa scale is 1 V/div and ordinate scale is 5 ns/div.

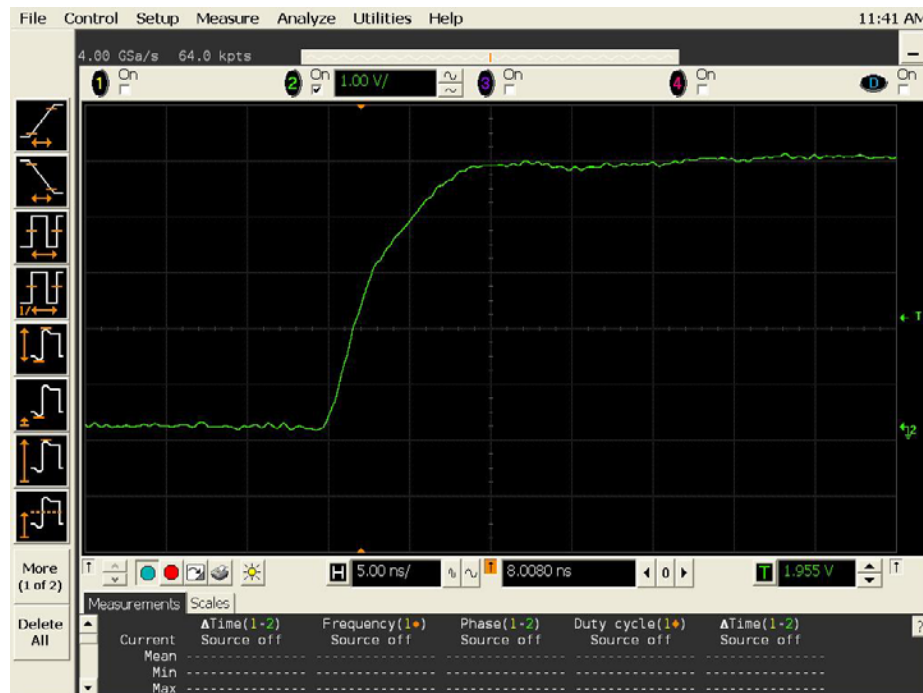


Figure 11a DUT 1369 Pre-Irradiation Rising Edge,
abscissa scale is 1 V/div and ordinate scale is 5 ns/div.

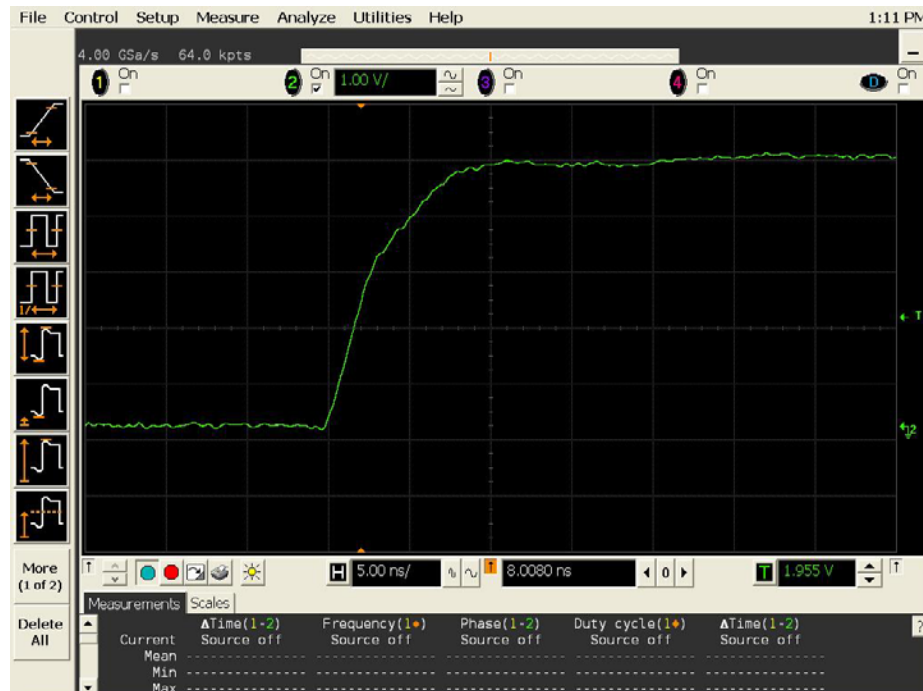


Figure 11b DUT 1369 Post-Annealing Rising Edge,
abscissa scale is 1 V/div and ordinate scale is 5 ns/div.

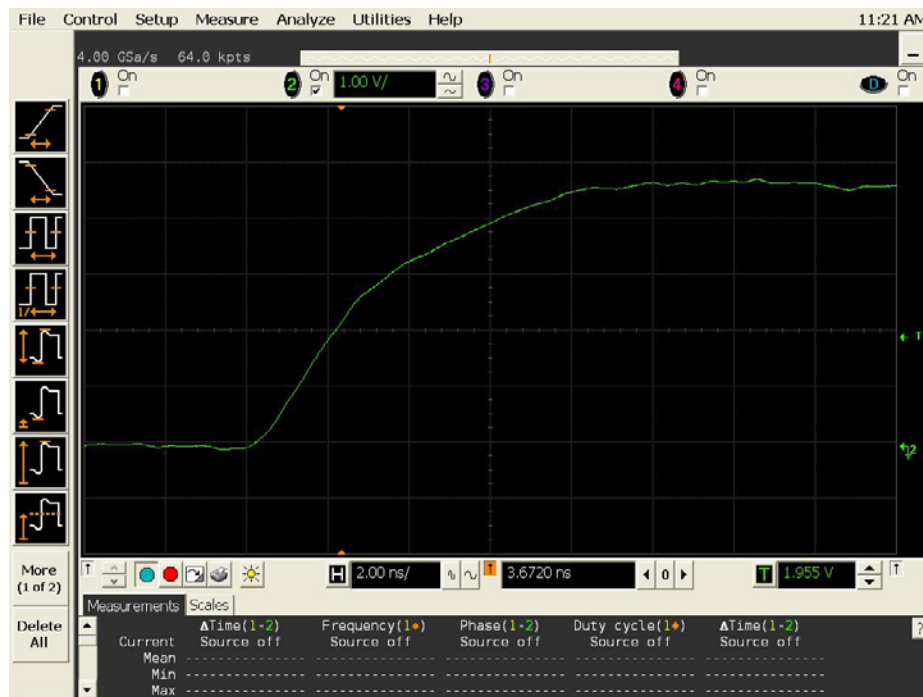


Figure 12a DUT 1413 Pre-Irradiation Rising Edge,
abscissa scale is 1 V/div and ordinate scale is 2 ns/div.

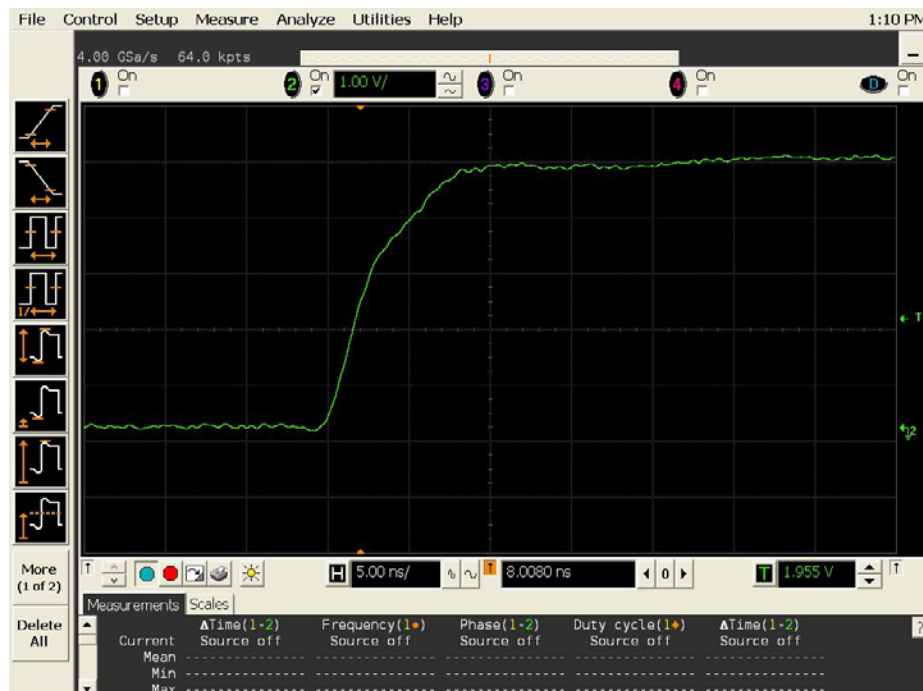


Figure 12b DUT 1413 Post-Annealing Rising Edge,
abscissa scale is 1 V/div and ordinate scale is 5 ns/div.



Figure 13a DUT 1301 Pre-Irradiation Falling Edge,
abscissa scale is 1 V/div and ordinate scale is 5 ns/div.

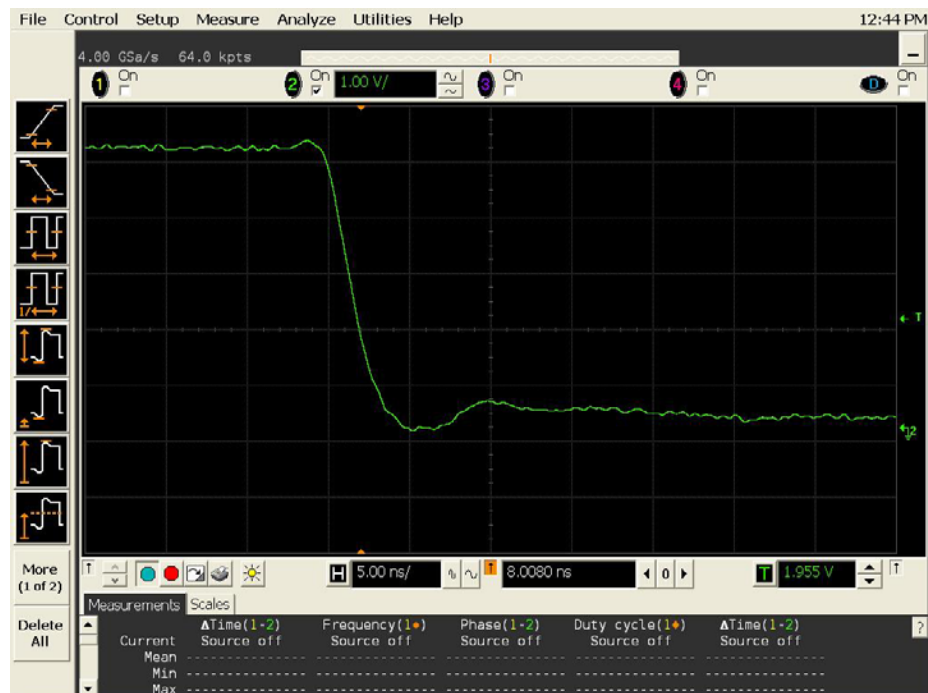


Figure 13b DUT 1301 Post-Annealing Falling Edge,
abscissa scale is 1 V/div and ordinate scale is 5 ns/div.

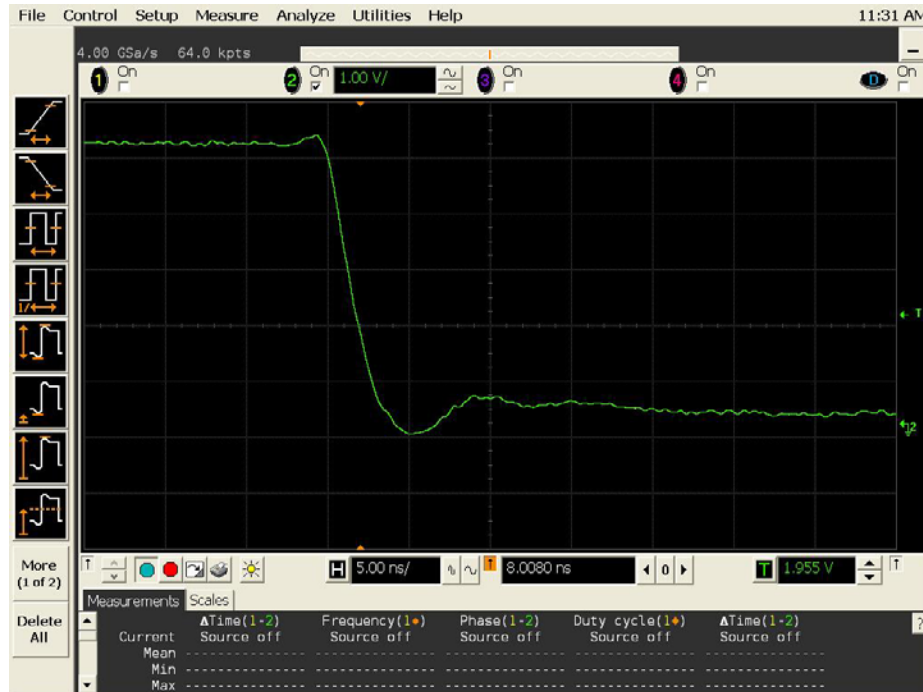


Figure 14a DUT 1328 Pre-Irradiation Falling Edge,
abscissa scale is 1 V/div and ordinate scale is 5 ns/div.

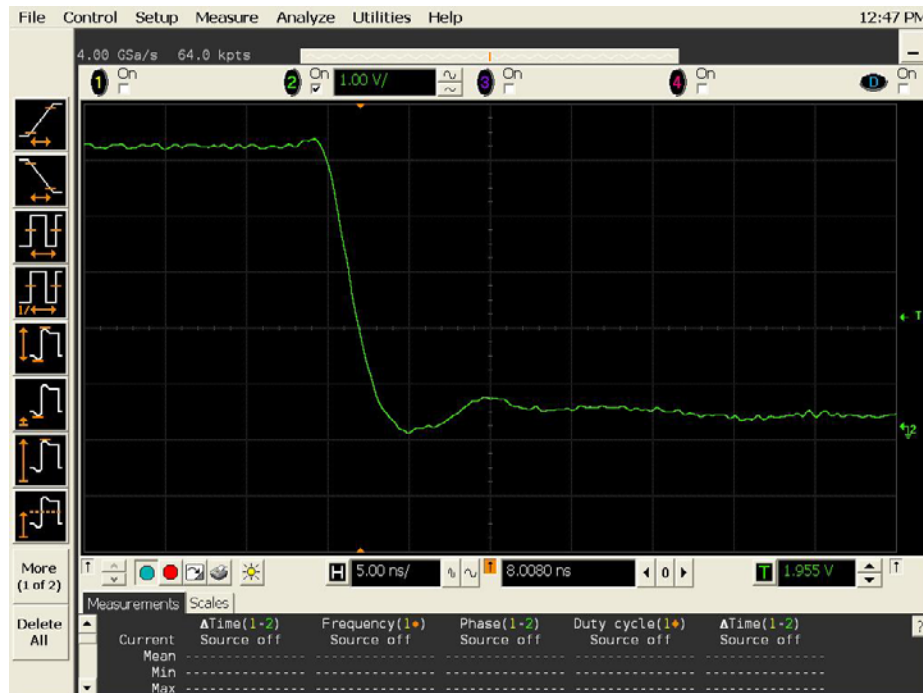


Figure 14b DUT 1328 Post-Annealing Falling Edge,
abscissa scale is 1 V/div and ordinate scale is 5 ns/div.

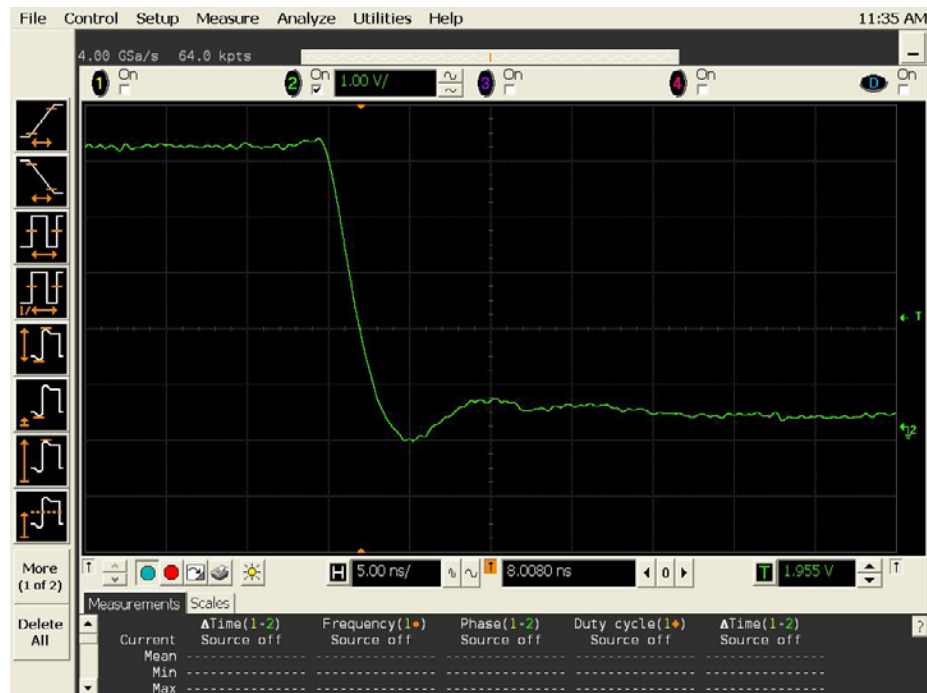


Figure 15a DUT 1342 Pre-Irradiation Falling Edge,
abscissa scale is 1 V/div and ordinate scale is 5 ns/div.

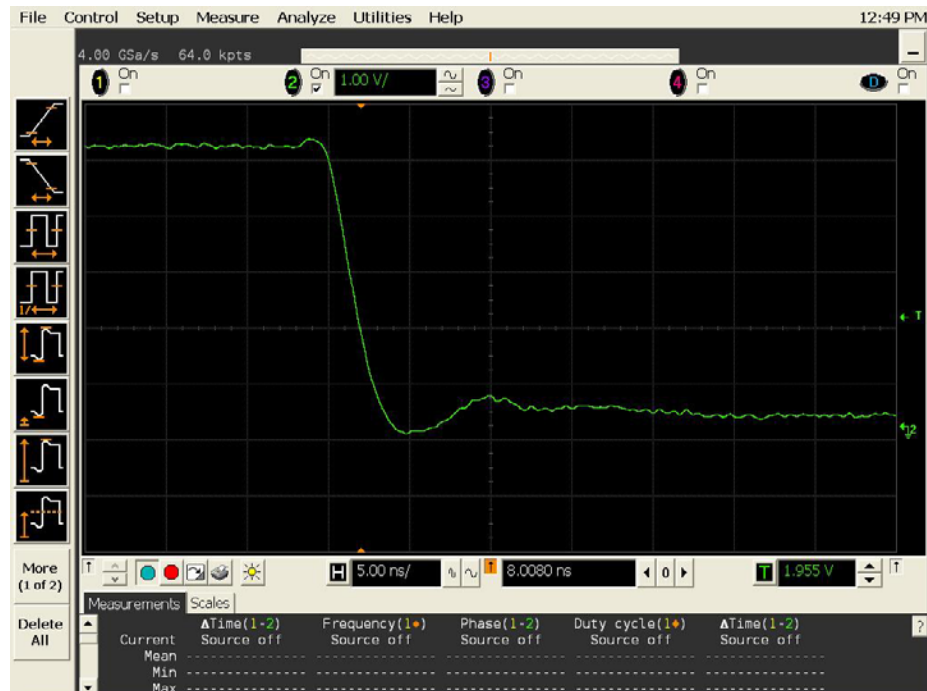


Figure 1(b) DUT 1342 Post-Annealing Falling Edge,
abscissa scale is 1 V/div and ordinate scale is 5 ns/div.

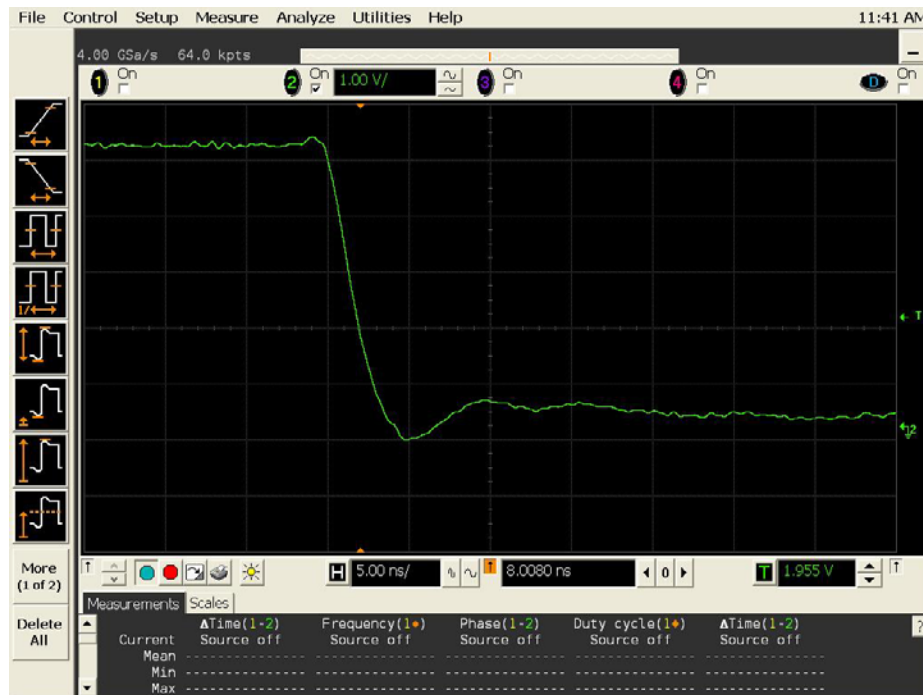


Figure 16a DUT 1369 Pre-Irradiation Falling Edge,
abscissa scale is 1 V/div and ordinate scale is 5 ns/div.

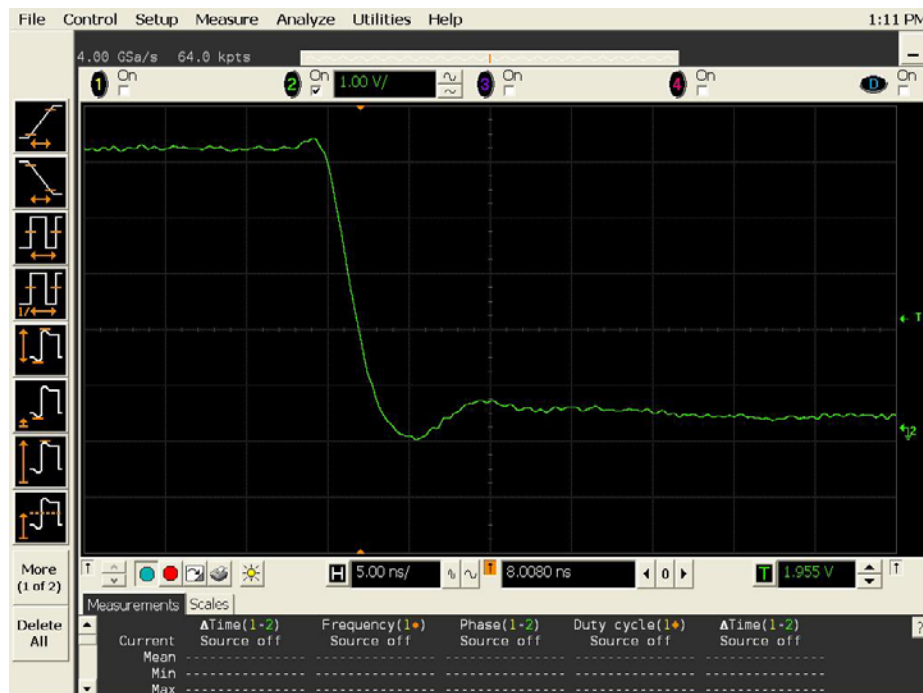


Figure 16b DUT 1369 Post-Annealing Falling Edge,
abscissa scale is 1 V/div and ordinate scale is 5 ns/div.

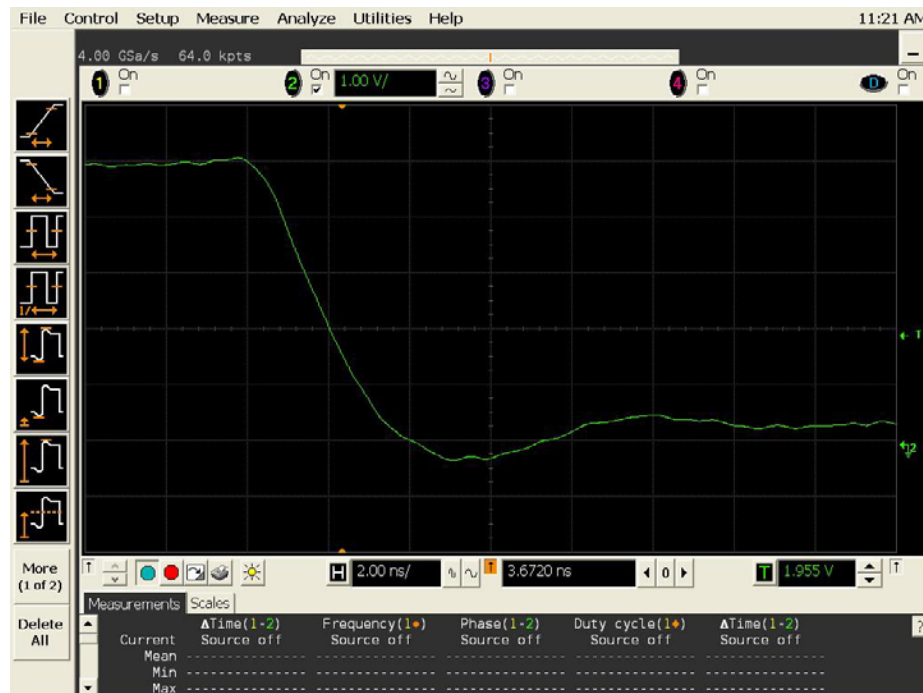


Figure 17a DUT 1413 Post-Annealing Falling Edge,
abscissa scale is 1 V/div and ordinate scale is 2 ns/div.

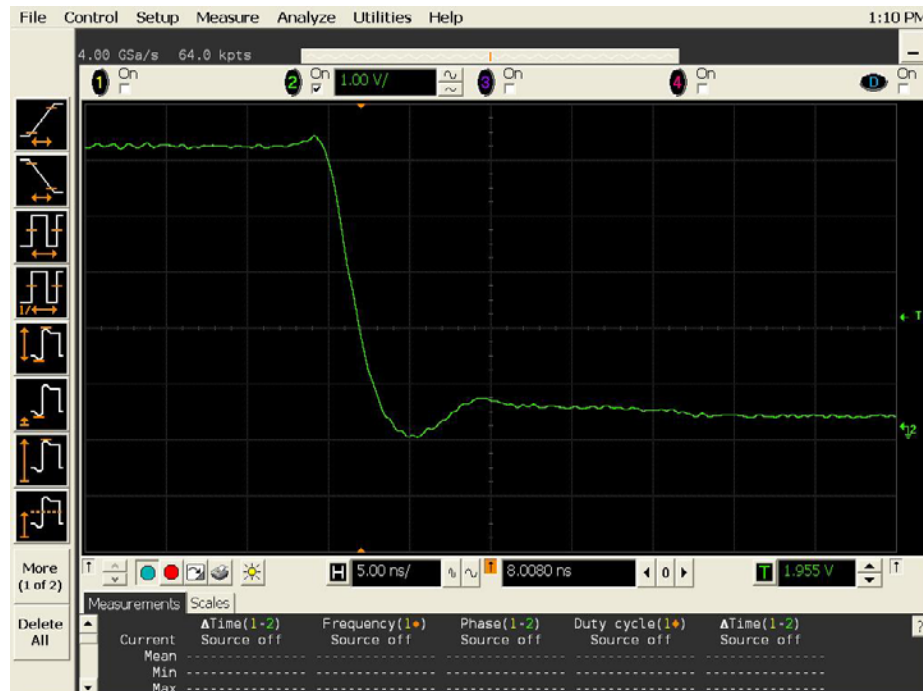


Figure 17b DUT 1413 Post-Annealing Falling Edge,
abscissa scale is 1 V/div and ordinate scale is 5 ns/div.



Microsemi Corporate Headquarters
2381 Morse Avenue, Irvine, CA 92614
Phone: 949.221.7100 · Fax: 949.756.0308
www.microsemi.com

Microsemi Corporation (NASDAQ: MSCC) offers the industry's most comprehensive portfolio of semiconductor technology. Committed to solving the most critical system challenges, Microsemi's products include high-performance, high-reliability analog and RF devices, mixed signal integrated circuits, FPGAs and customizable SoCs, and complete subsystems. Microsemi serves leading system manufacturers around the world in the defense, security, aerospace, enterprise, commercial, and industrial markets. Learn more at www.microsemi.com.

© 2011 Microsemi Corporation. All rights reserved. Microsemi and the Microsemi logo are trademarks of Microsemi Corporation. All other trademarks and service marks are the property of their respective owners.